J Appl Electrochem (2011) 41:787–793
DOI 10.1007/s10800-011-0296-x

ORIGINAL PAPER

Voltammetric studies of titanium (IV) phosphate modified with copper hexacyanoferrate and electroanalytical determination of *N*-acetylcysteine

Angelo Ricardo Fávaro Pipi · Devaney Ribeiro do Carmo

Received: 23 November 2010 / Accepted: 19 March 2011 / Published online: 1 April 2011

Abstract Titanium (IV) Phosphate copper hexacyanoferrate composite (TiPhCuHCF) was prepared using a new methodology for the synthesis. A preliminary characterization of the precursor and resulting materials was defined using spectroscopic and chemical techniques. The cyclic voltammogram of the modified electrode containing TiPhCuHCF exhibited two redox couples. The first and second redox couples present a formal potential ($E^{\theta'}$) of 0.18 and 0.76 V and were ascribed to the $Cu^{+/}Cu^{2+}$ $(E^{\theta'})_1$ and $Fe^{2+}(CN)_6/Fe^{3+}(CN)_6$ $(E^{\theta'})_2$ processes, respectively. In a preliminary study, the peak located at 0.76 V displays a sensitive response to *N*-acetylcysteine. The modified graphite paste electrode showed a linear range from 1.0×10^{-5} to 7.0×10^{-4} mol L^{-1} for the determination of *N*-acetylcysteine with a limit detection of 6.96×10^{-5} mol L^{-1} and relative standard deviation of $\pm$ 5% ($n = 3$) and amperometric sensitivity of 24.79×10^{-3} A mol L^{-1}. The modified electrode was electrochemically stable and showed good reproducibility.

Keywords Titanium (IV) phosphate · Cyclic voltammetry · *N*-acetylcysteine · Copper hexacyanoferrate · Composite

1 Introduction

Titanium dioxide is a widely used amphoteric inorganic material, which occurs in different structural types and can be used in many forms such as nanoparticles, sol–gels, nanofibers, and nanotubes [1–3]. It shows good biocompatibility, stability, and environmental safety. Most studies focus on different aspects, usually involving bio and photocatalytic activity fields [4–7] and a promising aspect is it use as an inorganic ion exchanger and sorbent [8, 9] due to its high chemical stability and high ion exchange capacity, which may find applications in solid phase extraction (SPE). An excellent review of investigations about the synthesis of nanopowders and films of titanium oxide for photocatalysis was recently published [10].

In the electrochemical field, the preparation of titanium chemically modified electrode surface has been a subject under active study in recent years. Various electrochemical methods are available for the preparation of TiO_2-based photocatalysts [11–16]. In general, the microstructured semiconductor oxides have often been used as a supporting matrix for electroactive species to form functionalized electrode materials [17]. Numerous ways for anchoring electrochemically active compounds onto electrode surfaces have been investigated aiming at shortening the distance between the redox sites involved in the electron transfer reaction. [18].

In this work, we report the voltammetric studies resulting from the direct preparation of Titanium (IV) Phosphate (TiPh) from aqueous phosphoric acid and Titanium (IV) isopropoxide. This method is characterized by its simplicity in composite preparation. TiPh has well-known ion exchange properties and good ionic conductor [19] and the combination will facilitate charge transfer between CuHCF and TiPh due to the cation diffusion within the CuHCF mediated by TiPh component. The material obtained from Titanium (IV) Phosphate (TiPh) was treated with Cu^{2+} (TiPhCu) and subsequent reaction with hexacyanoferrate to give rise to a new hybrid material

A. R. F. Pipi · D. R. do Carmo (✉)
Departamento de Física e Química, Faculdade de Engenharia de Ilha Solteira UNESP, Univ Estadual Paulista, Av. Brasil Centro, 56, Ilha Solteira, SP 15385-000, Brazil
e-mail: docarmo@dfq.feis.unesp.br

(TiPhCuHCF), which is a Prussian Blue analog, widely used for several applications. In this article, the novel material, after initial optimization conditions, was tested in the electrocatalysis of *N*-acetylcysteine.

2 Experimental

2.1 Reagents

All reagents were of analytical grade (p.a Merck) and used deionized water, Milli-Q Gradient system from Millipore. The solutions of *N*-acetylcysteine were prepared immediately before use.

2.2 Techniques

2.2.1 Fourier transform infrared spectra

Fourier transform infrared spectra were recorded on a Nicolet 5DXB FTIR 300 spectrometer. Approximately 600 mg of KBr was grounded in a mortar with a pestle, and a sufficient quantity of the solid sample was grounded with KBr to yield a 1 wt% mixture to produce KBr pellets. After the sample was loaded, the sample chamber was purged with nitrogen for at least 10 min prior to the data collection. A minimum of 32 scans was collected for each sample at a resolution of 4 cm^{-1}.

2.2.2 X-ray diffraction

The X-ray diffraction patterns (XRD) were obtained using a Siemens D 5000 diffractometer with Cu K_α radiation, submitted to 40 kV, 30 mA, 0.05°/s and exposed to radiation from 5 up to 30° (2θ).

2.2.3 Electrochemical measurements

For the cyclic voltammetric measurements, a potentiostat from Microchemistry was used, MQP1 model. A three-electrode system was used, which composed of: platinum electrode used as auxiliary, saturated calomel electrode (SCE) as a reference, and modified graphite paste as a working electrode. The working electrode consists of a 15-cm long glass tube, inner diameter of 0.30 cm, and external diameter of 0.5 cm, with the internal cavity connected by a copper wire to establish the electrical contact.

The cyclic voltammetry technique was employed to study the electrochemical behavior of titanium(IV) phosphate modified with copper hexacyanoferrate. The catalytic current was established by the difference between the current measured in the presence and absence of *N*-acetylcysteine. The solutions were bubbled with nitrogen for 10 min before the measurements.

2.3 Preparation of graphite paste electrode modified with TiPhCuHCF

The graphite paste modified with TiPhCuHCF was prepared from a mixture containing 20% (w/w) of 20 mg TiPhCuHCF with 80 mg graphite powder (Aldrich) and 30 μL of mineral oil.

2.4 Preparation of titanium (IV) modified with phosphoric acid (TiPh)

The synthesis of titanium phosphate was performed as described as follows: in a round-bottom flask 35 mL of phosphoric acid P.A.(85%), 20 mL of titanium isopropoxide (IV), and 10 mL of deionized water were added under strong agitation. The turbid solution formed was allowed to stand in the dark for 1 day. After the solid phase formed, it was separated by a sintered plate funnel and dried at room temperature. The material was stored in desiccators and described as TiPh.

2.5 Binuclear complex formation with the TiPh

The preparation of the binuclear complex was prepared in two steps; initially 2.0 g of TiPh was added into 25 mL of 1.0×10^{-3} mol L^{-1} Cu^{2+} solution. This mixture was stirred for 30 min at room temperature and the solid phase was then filtered and washed with deionized water several times, the prepared material was described as TiPhCu. In the second step, the TiPhCu was added to an aqueous solution containing 1.0×10^{-3} mol L^{-1} potassium ferricyanide ($K_3[Fe(CN)_6]$). The solution was stirred for 2 h then the precipitate was filtered, washed exhaustively with deionized water, and dried at room temperature. The material formed was described as TiPhCuHCF.

3 Results and discussion

The X-ray diffractogram of (TiPh) illustrated by Fig. 1, was analyzed by the Search-Match software in order to elucidate the crystalline characteristic of the compound formed in the new synthetic route proposed. The four intense peaks found in the diffractogram are located at 11.55°, 20.73°, 25.60°, and 35.72°. Through the XRD patterns analyzed by the software, it was concluded that these peaks are characteristic of the $Ti_3(PO_4)_4$ compound which form the Search-Match JCPDS database # 52-327.

Figure 2a shows the spectrum in the infrared region of TiPh, a broad band was detected in the region of

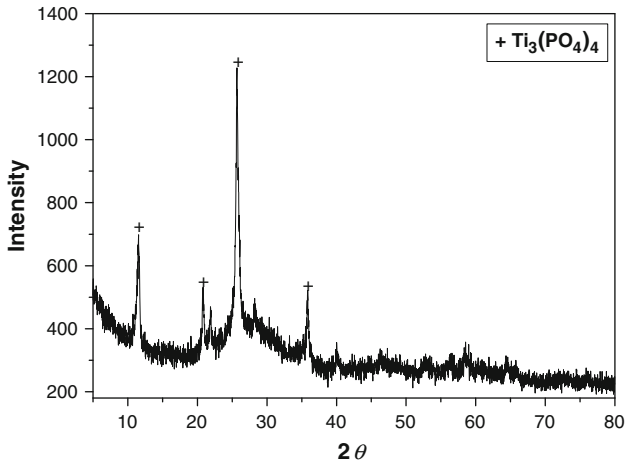

Fig. 1 X-ray diffractogram of titanium dioxide modified with phosphoric acid

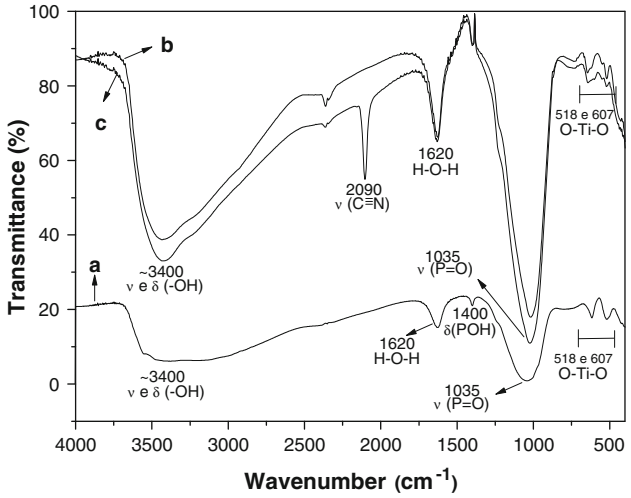

Fig. 2 Infrared spectrum of *a* TiPh, *b* TiPhCu, and *c* TiPhCuHCF

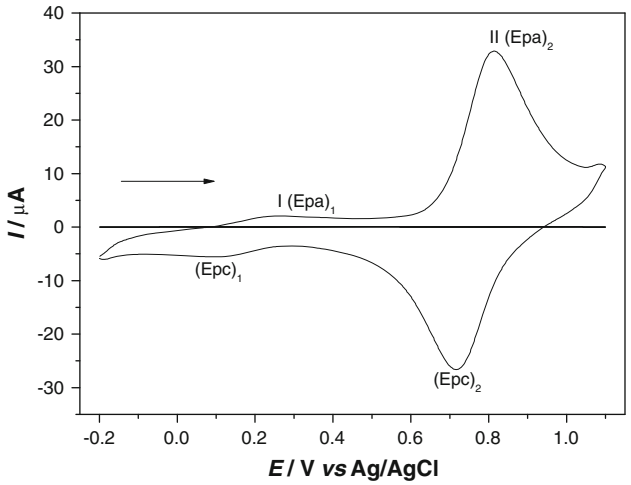

Fig. 3 Cyclic voltammogram of carbon paste modified with TiPCuFe ($v = 20$ mV s^{-1}, KCl 1.0 mol L^{-1})

3,400 cm^{-1} which was attributed to symmetrical and asymmetrical –OH stretch, there is also a narrow and medium band at 1,620 cm^{-1} that was assigned to the H–O–H bond in water and a strong absorption at 1,035 cm^{-1} which was attributed to ν (P=O) stretching. The band observed at 1,400 cm^{-1} was attributed to δ (POH) stretching [20]. The bands presented in the region 400–600 cm^{-1} with values of 518 and 607 cm^{-1} correspond to the O–Ti–O links [21]. These results suggest, in agreement with the X-ray diffraction patterns and those described in the literature [20], that the product formed by reaction of titanium isopropoxide with the phosphoric acid is the $Ti_3(PO_4)_4$. Figure 2b illustrates the infrared spectrum of TiPh after copper adsorption (TiPhCu) and the reaction between TiPhCu and hexacyanoferrate(III) potassium (TiPhCuHCF) shown in Fig. 2c. The spectra (b) and (c) showed the same peaks observed in spectrum (a) except for a peak at 2,090 cm^{-1} found only on the curve (c). This peak, assigned to ν (C≡N) stretching, shows the formation of copper hexacyanoferrate composite [22] formed at the surface of the starting material TiPh.

3.1 Electrochemical characterization of TiPhCuHCF

Figure 3 illustrates the cyclic voltammogram of TiPhCuHCF. Through the cyclic voltammogram of the modified electrode with carbon paste (20% m/m), a well-defined redox couple can be observed (peak II) with an average potential $(E^{\theta'})_2 = 0.76$ V which was attributed to the redox process $Fe^{2+}(CN)_6/Fe^{3+}(CN)_6$ of the binuclear complex formed, and another pair, with an undefined (peak I) and low-current intensity with $(E^{\theta'})_1 = 0.18$ V was attributed to the process Cu^{+}/Cu^{2+}. The last redox process is in concordance with observation verified by Kawana [23], in the same potential range.

3.2 Study on the effect of cations and anions

The oxidation and reduction process of the modified compounds on the TiPhCuHCF surface occurs initially by the equilibrium between the electrolyte solution cation and the electrode surface. The nature of the electrolyte solution cation that was used showed great influence on the current intensity and $(E^{\theta'})$. As illustrated in Fig. 4, studies performed with different cations showed that not only the current intensity as well as the average potential of redox couples of the two processes $(E^{\theta'})_1$ and $(E^{\theta'})_2$ are influenced by the cation nature, and these potentials are shifted to more anodic regions in the following sequence: $NH_4^+ > K^+ > Na^+ > Li^+$. Table 1 lists the main electrochemical parameters of the compounds mentioned above and their radii of hydration. Compounds such as Prussian Blue and similar structures that exhibit zeolitic cavity, in

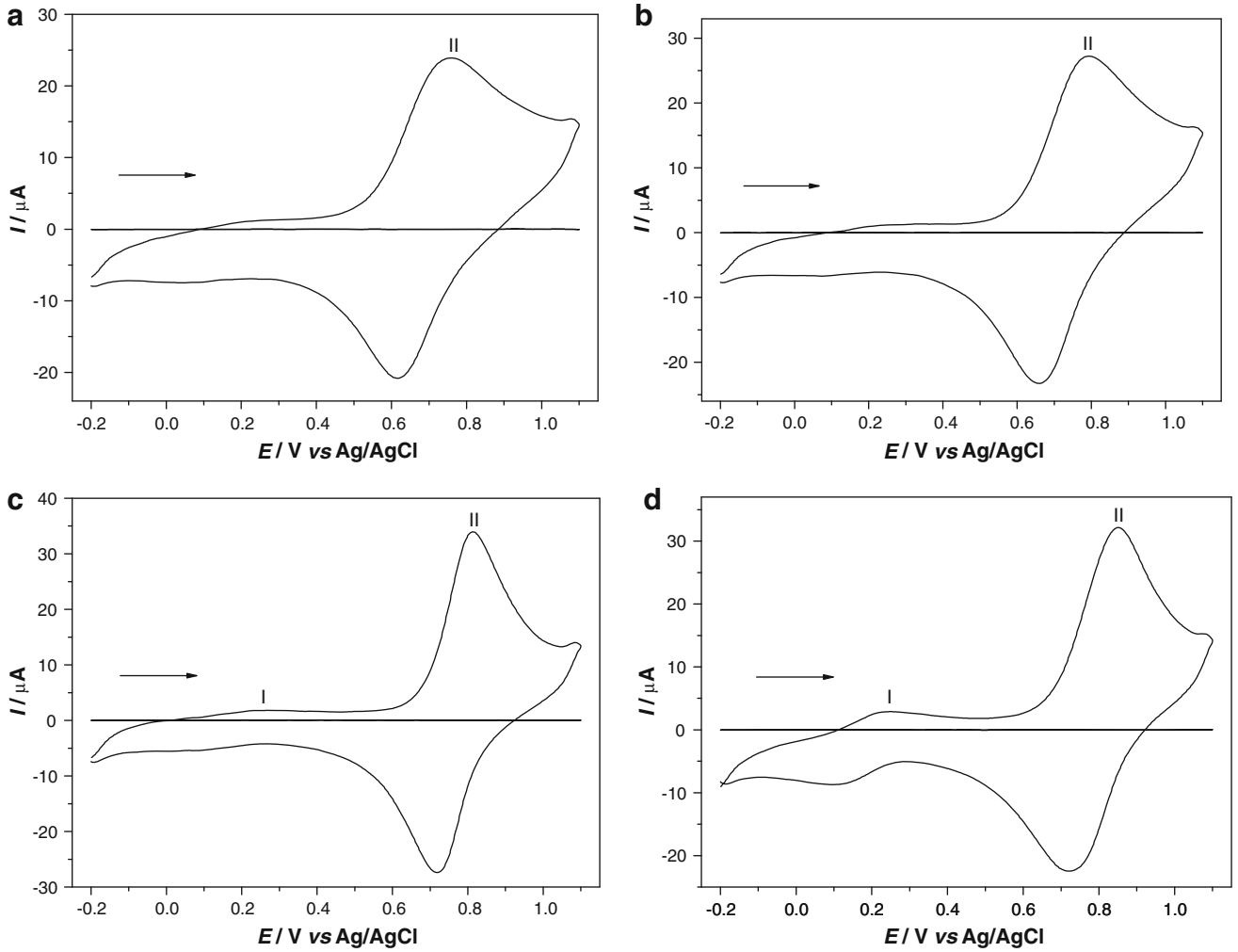

Fig. 4 Influence of the nature of cations in the graphite electrode modified with TiPCuFe: **a** LiCl, **b** NaCl, **c** KCl, **d** NH_4Cl (KCl 1.0 mol L^{-1}; $v = 20$ mV s^{-1})

other words, channels that allow the insertion of small molecules and ions behave as zeolites [24]. Since they have smaller hydration radii, K^+ and NH_4^+ are more easily lodged in the pores of the zeolite structure. Due to a higher affinity of these cations, as shown in the voltammograms of Fig. 5, there was a better electrochemical response of the electrode graphite paste modified with TiPhCuHCF in the presence of electrolyte containing cations K^+ and NH_4^+, the cation K^+ has a better voltammetric performance in relation to the cation NH_4^+, although almost the same hydrated radius, this can be explained by the cation NH_4^+ that has a low-ion mobility in relation to K^+ [24]. The cyclic voltammograms of carbon paste electrode modified with TiPhCuHCF recorded in the presence of different anions indicated that the two redox processes are not strongly influenced by the nature of the anion (Cl^-, NO_3^-, and SO_4^{2-}) (results not shown).

Figure 5 illustrates the cyclic voltammograms at different concentrations of KCl electrolyte solutions (1.0×10^{-3} to 2.0 mol L^{-1}), peak I showed a shift potential to more positive values with increasing concentration of electrolytes. Increasing the concentration of KCl showed the participation of the K^+ ion in the redox process, where the shift in potential is attributed to the change in the activity of these ions [25]. For the graphite paste electrode modified with TiPhCuHCF, the slope of this line was 53 mV per decade concentration of potassium ion concentrations, indicating a quasi Nernstian process [24]. Similar to the modified electrode with iron nitroprusside (Fe(II)NP) response where a quasi Nernstian behavior was an indication of the participation of potassium ions in the redox process. The dependence of the potential ($E^{\theta'}$) with the electrolyte concentration can be explained by the charge balance between the cation and TiPhCuHCF, similar results had been described in a previous publication to an analog compound copper nitroprusside (CuNP) [26].

Figure 6 shows the cyclic voltammogram at different pH values (2–8). With the increase in hydrogen ion

Table 1 Main voltammetric parameters of TiPhCuHCF in the presence of different supporting electrolytes

Cation	ΔEp_1 (*V*)	ΔEp_2 (*V*)	$(E^{\theta'})_1$ (*V*)	$(E^{\theta'})_2$ (*V*)	Diameter of the hydrated cation (nm)
Li^+	0.14	ND*	0.69	ND*	0.470
Na^+	0.13	ND*	0.73	ND*	0.360
K^+	0.09	0.18	0.76	0.16	0.240
NH_4^+	0.13	0.15	0.79	0.17	0.245

$\Delta Ep = Epa - Epc$

**ND* no detected,*Epa* anodic peak potential, *Epc* catodic peak potential

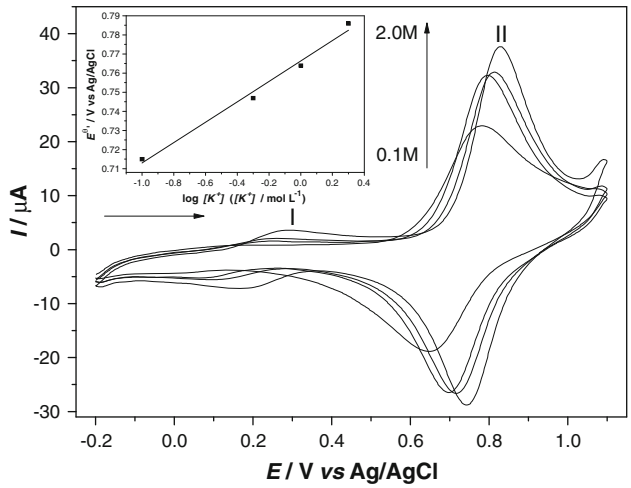

Fig. 5 Cyclic voltammogram of carbon paste electrode modified with TiPCuFe in several concentrations (0.1–2.0 mol L^{-1}). (*Inserted graphic* Average potencial ($E^{\theta'}$) of graphite paste modified with TiPCuFe as a function of log concentration of KCl)

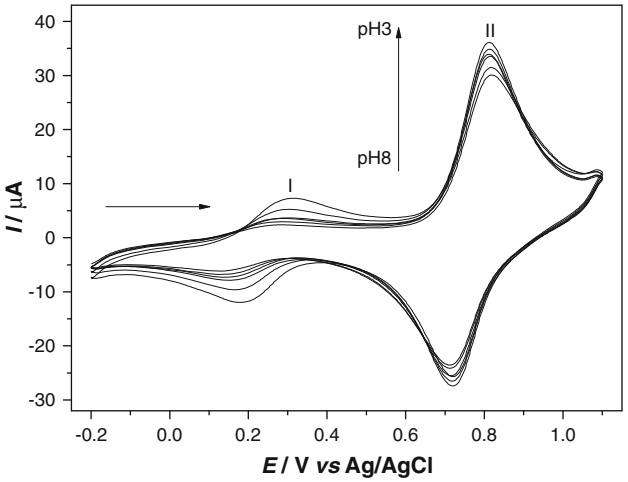

Fig. 6 Cyclic voltammogram of carbon paste modified with TiPCuFe to different pH values (3–8); (KCl 1.0 mol L^{-1}, $v = 20$ mV s^{-1})

concentration, there was a large increase in the current intensity for the redox process I (peak I; $(E^{\theta'})_1 = 0.18$ V) previously assigned to the Cu^+/Cu^{2+} redox couple. In the second process (peak II), the average potential ($(E^{\theta'})_2 = 0.76$ V) remained practically unchanged. Therefore, from pH < 4, the redox process (peak I) became more distinct, which can be explained by the presence of high concentrations of H^+ ions, which governs the electroactivity of one or more forms of intermediate species due a probable intercalation of H^+ ions into de metal hexacyanoferrates [24].

Figure 7 illustrates the cyclic voltammogram of TiPhCuHCF, respectively, at a different scan rate (10–100 mV s^{-1}). With increasing scan rate, we observed a linear dependence between the intensity of the anodic/cathodic peak current and the square root of the scan rate for peak II, thus characterizing a diffusion process [27].

Based on the results above, KCl (1.0 mol L^{-1}, pH 7.0) was chosen to be used in a subsequent voltammetric investigation. Figure 9 illustrates the performance of the graphite paste electrode with TiPhCuHCF in KCl solution 1.0 mol

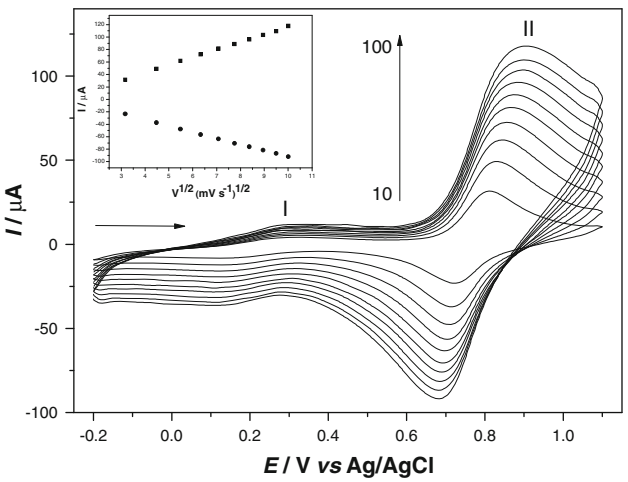

Fig. 7 Cyclic voltammogram of TiPCuFe at different scan rates: 10–100 mV s^{-1}; (KCl 1.0 mol L^{-1}; pH 7.0). (*Inserted graphic* Dependence of current peak II (anode and cathode) with the square root of the scan rate)

L^{-1}. The voltammogram in the absence (curve a) and presence (curve b) of 2.0×10^{-3} mol L^{-1} *N* acetylcysteine assigned to the bare graphite paste electrode showed no

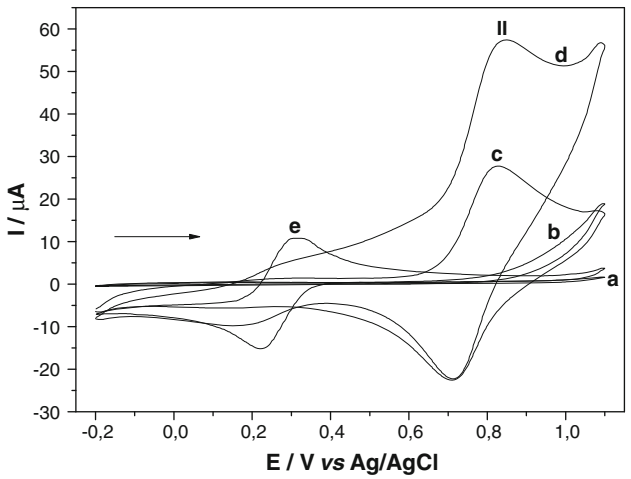

Fig. 8 Cyclic voltammogram of: *a* graphite paste electrode, *b* graphite paste electrode in 2.0×10^{-3} mol L^{-1} of *N*-acetylcysteine, *c* graphite paste electrode modified with TiPCuFe, *d* graphite paste electrode modified with TiPCuFe and 2.0×10^{-3} mol L^{-1} *N*-acetylcysteine; *e* graphite paste electrode without titanium phosphate plus 5.0×10^{-4} mol L^{-1} of $K_3Cu[Fe(CN)_6]$ (KCl 1.0 mol L^{-1}; $v = 20$ mV s^{-1})

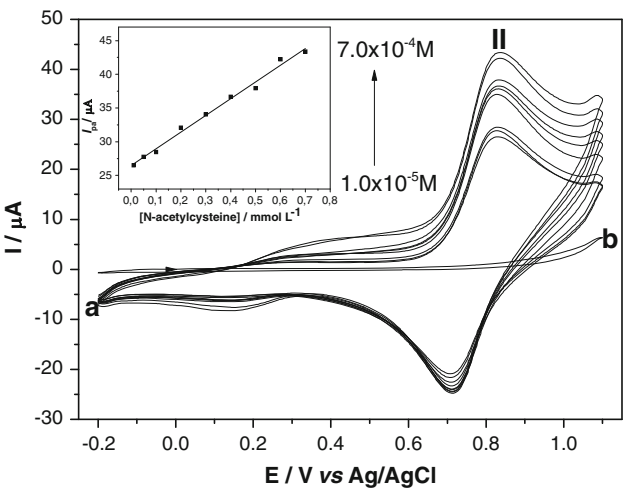

Fig. 9 Cyclic voltammograms of the applications of various concentrations of *N*-acetylcysteine using a graphite paste electrode modified : *a* with TiPCuFe : (*Inserted graphic* Analytical curve of the anodic peak for the determination of *N*-acetylcysteine using a graphite paste electrode modified with TiPCuFe; *b* graphite paste electrode without TiPCuFe in 1.0×10^{-5} mol L^{-1} *N*-acetylcysteine (KCl 1.0 mol L^{-1}, pH 7.0; v = 20 mV s^{-1})

electroactivity in the potential range studied (−0.2 to 1.1 V). The graphite paste electrode modified with TiPhCuHCF in the absence of *N*-acetylcysteine is shown in curve c. It was observed that in the presence of 2.0×10^{-3} mol L^{-1} of *N*-acetylcysteine the current of peak II increases as illustrated in curve d. In addition, the graphite paste electrode without titanium phosphate plus 5.0×10^{-4} mol L^{-1} of $K_3Cu[Fe(CN)_6]$ is showed in curve e. The intensity of the anodic peak current increases proportionally with the concentration of *N*-acetylcysteine as shown in Fig. 8. This increase occurs due to the electrocatalytic oxidation of *N*-acetylcysteine by the electron mediator TiPhCuHCF.

The equation for the electrochemical oxidation of L-cysteine as described in the literature [28] can be represented as follows:

$$2\text{L} - \text{cysteine(CySH)} \rightarrow \text{cystine (CySSCy)} + 2e^- + 2\,H^+ \quad (1)$$

Therefore, in view of this reaction of L-cysteine, the oxidation of *N*-acetylcysteine on the surface of the graphite paste electrode modified with TiPhCuHCF can be represented according to Eqs. 2, 3, and 4:

$$Ti\left(H_2PO_4^-\right)_4K_3Cu^+\left[Fe^{2+}(CN)_6\right] \rightleftarrows Ti\left(H_2PO_4^-\right)_4K_2Cu^{2+}\left[Fe^{2+}(CN)_6\right] + K^+ + e^-(0.26\ \text{V}) \quad (2)$$

$$Ti\left(H_2PO_4^-\right)_4K_2Cu^{2+}\left[Fe^{2+}(CN)_6\right] \rightleftarrows Ti\left(H_2PO_4^-\right)_4KCu^{2+}\left[Fe^{3+}(CN)_6\right] + K^+ + e^-(0.76\ \text{V}) \quad (3)$$

$$Ti\left(H_2PO_4^-\right)_4KCu^{2+}\left[Fe^{3+}(CN)_6\right] + 2X + 2K^+ \rightleftarrows Ti\left(H_2PO_4^-\right)_4K_3Cu^+\left[Fe^{2+}(CN)_6\right] + Y + 2\,H^+ \quad (4)$$

where X = *N*-acetylcysteine, Y = *N*-Acetylcystine.

Figure 9 illustrates the voltammogram when the concentration of *N*-acetylcysteine is changed. It was observed through these studies that the current for peak II ($(E^{0'})_1 = 0.76$ V) increases in accordance with the increase in concentration of the drug. Thus, it was determined that by adding aliquots of the *N*-acetylcysteine, the drug was oxidized by an electrocatalyst oxidation process on the electrode surface. The electrocatalytic oxidation of *N*-acetylcysteine occurs as follows: Fe^{3+} produced during the anodic scan, chemically oxidizes the molecule *N*-acetylcysteine when it is reduced to Fe^{2+}, which will again be electrochemically oxidized to Fe^{3+}.

Thus, *N*-acetylcysteine is oxidized at the electrode surface, and this process occurs in the potential of 0.76 V. The oxidation process does not occur in this potential when glassy carbon electrode or unmodified carbon paste is used. The peak potential is not affected by the concentration of *N*-acetylcysteine and the catalytic current is also linear with the square root of the scan rate. The behavior of electrochemical oxidation of *N*-acetylcysteine in the TiPhCuHCF modified electrode is very similar to the electrode modified with a film of Prussian blue, which shows an increase of the current in the two oxidation potentials (0.79 and 0.95 V) in the presence of *N*-acetylcysteine (1.0 mol L^{-1} KCl, pH 3.5 vs. Ag/AgCl) [29].

Figure 9 (inserted graphic) illustrates the analytical curve used to determine *N*-acetylcysteine. The modified electrode showed a linear response from 1.0×10^{-5} to 7.0×10^{-4} mol L^{-1} with the corresponding equation $Y(\mu A) = 24.79x + 26.469$ [*N*-acetylcysteine], and a correlation coefficient of $r = 0.9957$. The method showed a detection limit of 6.96×10^{-5} mol L^{-1} with a relative standard deviation of $\pm 5\%$ ($n = 3$) and amperometric sensitivity of 24.79×10^{-3} A mol L^{-1}.

4 Conclusion

Titanium (IV) Phosphate (TiPh) was prepared using a new methodology for the synthesis. The cyclic voltammogram of the modified electrode containing (TiPhCuHCF) exhibits two redox couples. The first and second redox couples present a formal potential ($E^{\theta'}$) of 0.18 and 0.76 v that were ascribed to Cu^{+}/Cu^{2+} $(E^{\theta'})_1$ and $Fe^{2+}(CN)_6/Fe^{3+}(CN)_6$ processes, respectively. The redox process presented by the graphite paste electrode modified with TiPhCuHCF $(E^{\theta'})_2 = 0.76$ V shows electrocatalytic activity for the oxidation of *N*-acetylcysteine. The linear range for the determination of *N*-acetylcysteine was found to be 1.0×10^{-5}–7.0×10^{-4} mol L^{-1}, showing a detection limit of 6.96×10^{-5} mol L^{-1} and amperometric sensitivity of 24.79×10^{-3}A mol L^{-1}.

The determination of *N*-acetylcysteine is a direct application of carbon paste electrode modified with TiPh-CuHCF. When compared to other electroanalytical methods, the main advantage of the modified electrode TiPhCuHCF is the manufacturing facility and the fact that its surface can be easily renewed. This is an important feature when one wants to effectively implement various measurements in a short period of time. Another advantage is that it needs no prior chemical treatment.

Acknowledgments This research was financially supported by Fundação de Amparo à Pesquisa do Estado de São Paulo (FAPESP-Proc.03/12882-6 and 07/57678-8).

References

1. Yao BD, Chan YF, Zhang XY, Zhang WF, Yang ZY, Wang N (2003) Appl Phys Lett 82:281–283
2. Fu GF, Vary PS, Lin CT (2005) J Phys Chem B 19:8889–8898
3. Yuan ZYU, Su BL (2004) Colloids Surf A 241:173–183
4. Zhang W, Zou L, Wang L (2009) Appl Catalysis A 371:1–9
5. Zielinska A, Kowalska E, Sobczak JW, Lacka I, Gazda M, Ohtani B, Hupka J, Zaleska A (2010) Sep Purif Technol 72:309–318
6. Lucky RA, Charpentier PA (2010) Appl Catalysis B 96:516–523
7. Akpan UG, Hameed BH (2010) Appl Catalysis A 375:1–11
8. Ma TY, Zhang XJ, Yuan ZY (2009) Microporous Mesoporous Mater 123:234–242
9. Ma TY, Zhang XJ, Shao GS, Cao JL, Yuan ZY (2008) J Phys Chem C 112:3090–3096
10. Shapovalov VI (2010) Glass Phys Chem 36:121–157
11. Song W, Xiaohong W, Wei Q, Zhaohua J (2007) Electrochim Acta 53:1883–1889
12. Karuppuchamy S, Suzuki N, Ito S, Endo T (2009) Curr Appl Phys 9:243–248
13. Fan L, Ichikuni N, Shimazu S, Uematsu T (2003) Appl Catalysis A 246:87–95
14. Chen J, Zhang J, Xian Y, Ying X, Liu M, Jin L (2005) Water Res 39:1340–1346
15. Takahashi M, Tsukigi K, Uchino T, Yoko T (2001) Thin Solid Film 388:231–236
16. Kumar SA, Lo PH, Chen SM (2008) Nanotechnology 19: 255501–255508
17. McKenzie KJ, Marken F (2003) Langmuir 19:4327–4331
18. Willner I, Katz E (2000) Angew Chem Int Ed Engl 39:1180–1218
19. Wang Q, Zhang L, Qiu L, Sun J, Shen J (2007) Langmuir 23: 6084–6090
20. Costa ACFM, Vilar MA, Lira HL, Kiminami RHGA, Gama L (2006) Cerâmica 52:255–259
21. Thakkar R, Chudasama U (2009) Electrochim Acta 54:2720–2726
22. Los-Neskovic C, Ayrault S, Badillo V, Jimenez B, Garnier E, Fedoroff M, Jones DJ, Merinov B (2004) J Solid State Chem 177:1817–1828
23. Siperko LM, Kuwana T (1983) J Electronchem Soc 130:396–402
24. Do Carmo DR, Silva RM, Stradiotto NR (2002) Ecletica Quim 27:197–210
25. Do Carmo DR, Silva RM, Stradiotto NR (2005) Port electrochim Acta 23:457–470
26. Baiani AP, Vidotti M, Fiorito PA, Torresi SIC (2008) J Electroanal Chem 119:135–142
27. Bard AJ, Faulkner LR (1980) Electrochemical methods. Wiley, New York
28. Ralph TR, Hitchman ML, Millington JP, Walsh FC (1994) J Electroanal Chem 375:1–15
29. Hou W, Wang E (1991) J Electroanal Chem 316:155–163